# Rho-Kinase–mediated Contraction of Isolated Stress Fibers✪

**Kazuo Katoh,* Yumiko Kano,* Mutsuki Amano,‡ Hirofumi Onishi,* Kozo Kaibuchi,‡§ and Keigi Fujiwara*‖**

*Department of Structural Analysis, National Cardiovascular Center Research Institute, Suita, Osaka 565-8565, Japan; ‡Division of Signal Transduction, Nara Institute of Science and Technology, Ikoma, Nara 630-0101, Japan; §Department of Cell Pharmacology, Nagoya University School of Medicine, Showa, Nagoya, Aichi 466-8550, Japan; and ‖Center for Cardiovascular Research, University of Rochester, Rochester, New York 14642

***Abstract.*** It is widely accepted that actin filaments and the conventional double-headed myosin interact to generate force for many types of nonmuscle cell motility, and that this interaction occurs when the myosin regulatory light chain (MLC) is phosphorylated by MLC kinase (MLCK) together with calmodulin and $Ca^{2+}$. However, recent studies indicate that Rho-kinase is also involved in regulating the smooth muscle and nonmuscle cell contractility. We have recently isolated reactivatable stress fibers from cultured cells and established them as a model system for actomyosin-based contraction in nonmuscle cells. Here, using isolated stress fibers, we show that Rho-kinase mediates MLC phosphorylation and their contraction in the absence of $Ca^{2+}$. More rapid and extensive stress fiber contraction was induced by MLCK than was by Rho-kinase. When the activity of Rho-kinase but not MLCK was inhibited, cells not only lost their stress fibers and focal adhesions but also appeared to lose cytoplasmic tension. Our study suggests that actomyosin-based nonmuscle contractility is regulated by two kinase systems: the $Ca^{2+}$-dependent MLCK and the Rho-kinase systems. We propose that $Ca^{2+}$ is used to generate rapid contraction, whereas Rho-kinase plays a major role in maintaining sustained contraction in cells.

Key words: Rho • Rho-kinase • stress fiber • contraction • myosin regulatory light chain

## *Introduction*

Ras homology (Rho)[1] proteins are GTPases involved in signal transduction and form a subfamily within the Ras superfamily. Whereas Ras functions on the plasma membrane, Rho proteins work at various sites within the cell. Its role in the regulation of cell motility and cytoskeletal organization is a target of intense studies in recent years (Ridley and Hall, 1992; Takai et al., 1995; Hall, 1998; Amano et al., 2000). The active form of Rho is GTP bound (Van Aelst and D'Souza-Schorey, 1997; Hall, 1998), and many polypeptides have been reported as targets of activated Rho, including Rho-kinase/ROKα/ROCK II (Isenberg et al., 1976; Leung et al., 1995; Matsui et al., 1996), myosin-binding subunit (MBS) of myosin phosphatase (Kimura et al., 1996), p140mDia (Watanabe et al., 1997), protein kinase N (Amano et al., 1996b), and phospholipase D (Singer et al., 1997). RhoA is a Rho protein expressed in most, if not all, of the cell. When cultured cells are treated with LPA or bombesin, new stress fibers and focal adhesions are formed in the cells (Ridley and Hall, 1992, 1994). This response appears to be mediated by RhoA because (a) both LPA and bombesin activate RhoA and (b) microinjection of active RhoA into cultured cells induce the formation of stress fibers and focal adhesions (Ridley and Hall, 1992).

Rho proteins activate Rho-kinase, which consists of four domains: catalytic, coiled coil (CC), Rho-binding (RB), and pleckstrin homology domains. The recombinant catalytic domain acts as constitutively active Rho-kinase (Amano et al., 1997). Recent studies have shown that Rho-kinase phosphorylates the myosin regulatory light chain (MLC) of smooth muscle (Amano et al., 1996a; Kureishi et al., 1997) and of fibroblast (Chihara et al., 1997; Amano et al., 1998) myosins. This Rho-kinase–dependent MLC phosphorylation induced contraction of permeabilized smooth muscle cells. Myosin phosphatase is

✪The online version of this article contains supplemental material.

Address correspondence to Kazuo Katoh, Department of Structural Analysis, National Cardiovascular Center Research Institute, 5 Fujishirodai, Suita, Osaka 565, Japan. Tel.: 81-6-6833-5012 ext. 2508. Fax: 81-6-6872-8092. E-mail: katoichi@ri.ncuc.go.jp

[1]*Abbreviations used in this paper:* CC, coiled coil; GFP, green fluorescent protein; GST, glutathione *S*-transferase; MBS, myosin-binding subunit; MLC, myosin regulatory light chain; MLCK, MLC kinase; RB, Rho-binding; Rho, Ras homology; TEA, triethanolamine (2, 2′, 2″-nitrilotriethanol).

another regulatory protein for smooth muscle and nonmuscle contraction. It consists of three subunits: a 110-kD MBS, a 37-kD catalytic subunit, and a 20-kD regulatory subunit (Alessi et al., 1992; Hartshorne et al., 1998). Its role is to dephosphorylate MLC, terminating the actomyosin-based contraction. In vitro experiments have demonstrated that Rho-kinase phosphorylates MBS and inhibits the activity of myosin phosphatase (Kimura et al., 1996; Kawano et al., 1999). Thus, Rho-kinase can promote actomyosin contraction in two ways: one by directly activating myosin and the other by inactivating myosin phosphatase. These Rho-kinase activities do not depend on $Ca^{2+}$/calmodulin.

Stress fibers are present in many types of cultured cells as well as certain types of cells in situ (Buckley and Porter, 1967; Byers et al., 1984). Recently, we have succeeded in isolating stress fibers from cultured cells and reactivated them with Mg-ATP in the presence of $Ca^{2+}$ (Katoh et al., 1998). This contraction was inhibitable by MLC kinase (MLCK) inhibitors. There are several other actomyosin-based nonmuscle contractile model systems, such as the extracted cell model (Hoffmann-Berling, 1954; Isenberg et al., 1976; Kreis and Birchmeier, 1980), the isolated brush border (Mooseker and Tilney, 1975; Rodewald et al., 1976), and the circumferential marginal band (Owaribe and Masuda, 1982). Reactivation of all of these models requires $Ca^{2+}$ and ATP, suggesting that their contraction is mediated by MLCK. Interestingly, most of these models as well as our isolated stress fiber model are made using Triton X-100.

Here, we show that a stress fiber model prepared using glycerol instead of Triton X-100 is capable of contracting both in the presence and absence of $Ca^{2+}$ and that the $Ca^{2+}$-independent contraction is mediated by Rho-kinase. We found that extraction of cells and stress fibers with Triton X-100 readily solubilized both RhoA and Rho-kinase, and that such stress fibers showed $Ca^{2+}$-dependent contraction only. However, when dominant-active Rho-kinase was added to the Triton X-100 extracted stress fibers, $Ca^{2+}$-independent contraction was recovered. Our study appears to indicate that tension production within stress fibers is achieved by both $Ca^{2+}$-dependent and -independent systems. To gain insights into the role of MLCK and Rho-kinase in normal interphase cells, fibroblasts transfected with green fluorescent protein (GFP)–actin were treated with specific inhibitors. GFP–actin-transfected cells exhibited well-developed stress fibers. When these fibroblasts were treated with Y-27632, a Rho-kinase inhibitor, stress fibers and focal adhesions were disrupted, and in addition, cells appeared to lose tension. These observations suggest that Rho-kinase is involved in not only the formation/maintenance of stress fibers and focal adhesions as shown by others (Ridley and Hall, 1992) but also the regulation of cytoplasmic tension in the cell. It is not clear in what way Rho-kinase activity is involved in formatting/maintenance of stress fibers and focal adhesions. However, since contraction is a much quicker response than the formation of focal adhesions and stress fibers, it is possible that the new assembly of these structures may not be the direct effect of RhoA but is the result of cellular contraction induced by RhoA activating Rho-kinase.

## Materials and Methods

### Cell Culture

Human foreskin fibroblasts (FS-133) were cultured by using a 1:1 mixture of Dulbecco's modified eagle's medium and a nutrient mixture F-12 (GIBCO BRL), pH 7.4, containing 50 U/ml penicillin, 50 μg/ml streptomycin, and 10% fetal bovine serum (Salmond Smith Biolab) (Sunada et al., 1993). The cells were maintained at 37°C in a humidified 5% $CO_2$ atmosphere.

### Isolation of Stress Fibers

Stress fibers were isolated by a modified method described in our previous reports (Katoh et al., 1998, 2000). In brief, FS-133 grown for 3–4 d in culture dishes (150 mm in diameter) (Greiner) or on coverslips were briefly washed in an ice-chilled PBS and then extracted for 20–30 min with gentle agitation in a low ionic strength solution consisting of 2.5 mM triethanolamine (2, 2', 2"-nitrilotriethanol) (TEA), 20 μg/ml trasylol (Bayer), 1 μg/ml leupeptin (Peptide Institute), and 1 μg/ml pepstatin (Peptide Institute), pH 8.2, at 4°C. At this stage, most cells lost their dorsal side and nuclei, but some still had these parts of the cell, which could be removed by gentle shearing under a phase–contrast microscope with a stream of extraction buffer. The material attached to culture dishes or coverslips were gently washed by Triton X-100–based extraction buffer (0.05% Triton X-100 [Wako], 20 μg/ml trasylol, 1 μg/ml leupeptin, and 1 μg/ml pepstatin in PBS, pH 7.4) for 3–30 min. Still attached to culture dishes or coverslips were mainly stress fibers (model 1), and such preparations were used for protein localization and contraction studies. We also made a glycerol-extracted stress fiber model (model 2). The TEA-extracted material was treated with PBS containing 50% glycerol, 20 μg/ml trasylol, 1 μg/ml leupeptin, and 1 μg/ml pepstatin, pH 7.4 (glycerol extraction buffer) for 5 min. During this extraction period, the material on culture dishes or coverslips was sheared with a stream of the glycerol extraction buffer while observing under a phase–contrast microscope.

For immunoblotting and autoradiography analyses, the Triton X-100–extracted stress fibers (model 1) were mechanically detached from culture dishes and collected by centrifugation at 100,000 *g* for 1 h. The pellet contained isolated stress fibers sufficient for biochemical analyses.

### Antibodies

Polyclonal antibodies against the chicken gizzard MLC was previously made (Onishi et al., 1995). The following monoclonal antibodies were purchased: anti–α-smooth muscle actin (Sigma-Aldrich), antimyosin (Amersham Pharmacia Biotech), anti-MLCK (Sigma-Aldrich), anti-MLC (Sigma-Aldrich), antivinculin (Sigma-Aldrich), antivimentin (Sigma-Aldrich), and anti-RhoA (Santa Cruz Biotechnology, Inc.; Transduction Laboratories). Polyclonal anti-RhoA was also purchased (Santa Cruz Biotechnology, Inc.). A rabbit affinity-purified polyclonal antibody against the glutathione *S*-transferase (GST)–bound MBS peptide (GST-MBS-N; amino acids 1–706) was already described (Kawano et al., 1999). A rabbit polyclonal antibody against MBS phosphorylated at Ser-854 (anti-pS854 antibody), which recognizes the phosphorylated form of MBS, was previously described (Inagaki et al., 1997; Kawano et al., 1999). Two rabbit polyclonal antibodies against Rho-kinase were generated using the GST-fused CC domain (amino acids 421–701) and the GST-fused RB domain (amino acids 941–1075) of bovine Rho-kinase (Matsui et al., 1996).

### Preparation of Recombinant Proteins

Dominant-active Rho-kinase was the catalytic domain (amino acids 6–553) of the kinase without the RB and the Ph domains of Rho-kinase expressed as a GST fusion protein in *Spodoptera frugiperda* cells using a baculovirus system (Amano et al., 1996a). Dominant-negative Rho-kinase was a polypeptide, containing the RB and the Ph domains of Rho-kinase (amino acids 941–1388), in which 1027 Asn and 1028 Lys were substituted by threonines (Amano et al., 1998). This Rho-kinase fragment did not contain the catalytic domain and was expressed as a maltose-binding protein fusion protein in *Escherichia coli*.

### Immunofluorescence Microscopy

Stress fiber models and cells were fixed with 1% paraformaldehyde in PBS for 30–60 min and treated with 10% normal goat serum for 1 h at room temperature. They were then stained with anti-RhoA (dilution

1:100), anti-MLCK (1:100), anti-MLC (1:100 for monoclonal, 1:1,000 for polyclonal), antimyosin (1:100), antivimentin (1:100), anti–Rho-kinase (1:200), anti–Rho-kinase (CC) (1:200), anti-MBS (1:100) or anti–phosphorylated MBS (pS854)(1:50) for 60 min. After being washed in PBS, samples were incubated with fluorescein- (Cappel), rhodamine- (Cappel), or Texas red–labeled (EY-Lab) goat anti–rabbit or anti–mouse IgG. Some specimens were double stained with one of the antibodies (and the appropriate secondary antibody) and rhodamine- (Molecular Probes) or fluorescein-labeled (Sigma-Aldrich) phalloidin.

Specimens were observed using an Axiophot (Carl Zeiss, Inc.) epifluorescence microscope with an apochromat 63× (NA 1.4, oil) objective lens. Fluorescent images were photographed by using Kodak® T-Max 400 film (Eastman Kodak Co.).

### SDS-PAGE and Immunoblotting

Crude extracts and Triton X-100–insoluble fractions (extraction by 0.1% Triton X-100 in PBS for 10 min) of human foreskin fibroblasts, Triton X-100 extracted stress fiber preparations (model 1 stress fibers: TEA for 20 min, Triton X-100 for 30 min), and glycerol extracted stress fiber models (model 2 stress fibers: TEA for 30 min, glycerol 5 min) were made. Protein concentrations were determined by using a Micro BCA Protein Assay kit (Pierce Chemical Co.). Samples were boiled for 3 min in the SDS-PAGE sample buffer, and 2 μg of protein from each sample were electrophoresed on 10% polyacrylamide gels according to the method of Laemmli (1970). Gels were stained using a silver staining kit (Wako). For immunoblotting, 10 μg of protein were loaded in each lane, and polypeptide bands in an SDS-PAGE gel were electrophoretically transferred to a piece of nitrocellulose paper (Millipore; 0.45 μm pore size). The paper was treated with 10% nonfat dry milk in TBS, pH 7.4, and then incubated with anti-MBS (dilution 1:1,000), anti–phosphorylated MBS (1:500), polyclonal anti-MLC (1:500), anti–Rho-kinase (1:500), anti–α-smooth muscle actin (1:200), anti-MLCK (1:500), or anti-RhoA (1:1,000). Filter papers were washed in TBS and further incubated with a horseradish peroxidase conjugated secondary antibody or an avidin–biotin complex system (Vector Laboratories). Immunoreacted bands were visualized by using an ECL kit (Amersham Pharmacia Biotech).

To examine RhoA and Rho-kinase extraction from stress fibers by Triton X-100, the same number of cells were plated on culture dishes (10 mm in diameter) and treated with TEA buffer for 30 min. They were then extracted by Triton X-100–containing buffer for 0, 0.5, 1, 3, 4, 5, 10,15, 20, and 30 min and analyzed by immunoblotting with anti-RhoA, anti–Rho-kinase, and anti–α-smooth muscle actin.

### Contraction of Stress Fibers

Stress fiber models in a perfusion chamber (Katoh et al., 1998) were first immersed in a wash solution (10 mM imidazole, 100 mM KCl, and 2 mM EGTA) and perfused with a Mg-ATP solution (0.1 mM ATP, 3 mM MgCl, 1 mM EGTA, 75 mM KCl, 20 mM imidazole, pH 7.2) with or without 1 mM $CaCl_2$. For $Ca^{2+}$-independent stress fiber contraction experiments, model 1 stress fibers were perfused with $Ca^{2+}$-free Mg-ATP solution with dominant-active Rho-kinase (5.1 μg/ml) or dominant-negative Rho-kinase (5–50 μg/ml). Some samples were perfused with $Ca^{2+}$-free Mg-ATP solution with 10 μM microcystin LR (Biomol), a phosphatase inhibitor. Contraction was observed under a phase–contrast microscope (Axiophot with a plan-neofluar 63×, NA 1.25, oil, antiflex objective lens; Carl Zeiss, Inc.) equipped with a video-enhanced imaging system for 5–20 min. The video system consisted of a high resolution charge-coupled device camera (C2400-77; Hamamatsu Photonics) and a digital image processor (Image Sigma-II; Nippon Avionics), and images were recorded by a high resolution laser video disk recorder (LV-250H; TEAC).

### Phosphorylation of MLC

To study the effect of MLC phosphorylation on stress fiber contraction, isolated stress fibers or stress fiber models were incubated in a solution containing 0.1 mM [γ-$^{32}$P]ATP (7.4 gigabecqueral/mM) (Amersham Pharmacia Biotech), 3 mM $MgCl_2$, 1 mM $CaCl_2$, 1 mM EGTA, 75 mM KCl, and 20 mM imidazole, pH 7.2, under various conditions. Some of the stress fiber samples were pretreated with 10 μM wortmannin (Wako), an MLCK inhibitor, in 75 mM KCl, 3 mM $MgCl_2$, 1 mM $CaCl_2$, 1 mM EGTA, 20 mM imidazole, pH 7.2, for 30 min or more on ice. Certain specimens were also pretreated with 1–10 μM HA1077 (Takayasu et al., 1986; Uehata et al., 1997), provided by Asahi Chemical Industry in 75 mM KCl, 3 mM $MgCl_2$, 1 mM $CaCl_2$, 1 mM EGTA, 20 mM imidazole, pH 7.2, for 30 min or more on ice. MLC phosphorylation was determined autoradiographically by using a BAS-5000 image analyzer (Fuji Film). Phosphorylation of MLC was also determined by urea gel electrophoresis. Model 1 stress fibers alone and model 1 stress fibers incubated with Mg/ATP containing $Ca^{2+}$ were electrophoresed, and the bands were visualized by silver staining (Wako). Purified chicken gizzard MLC (unphosphorylated) was used as control. 10 μg of protein were loaded in each lane.

### GFP–Actin Expression in Human Foreskin Fibroblast

Human foreskin fibroblasts (FS-133) were transfected with the pEGFP–actin vector (CLONTECH Laboratories, Inc.) using the Tfx™-50 reagents (Promega). Transfected cells were cultured as described above. For time-lapse confocal laser scanning microscopy, GFP–actin-transfected cells were plated on a culture dish (5 cm in diameter) and placed on a temperature-controlled stage at 37°C (Tokai). Culture medium was exchanged every 20 min for long-term observations. For inhibitor experiments, Y-27632 (Uehata et al., 1997) provided by Yoshitomi Pharmaceutical Industry (10 μM), HA1077 (30 μM), wortmannin (100 nM), ML-7 (25 μM), or KT5926 (15 μM) was added to culture medium. Samples were observed under a confocal laser scanning fluorescence microscope (Fluoview with a LUMPlanFl 60×, NA 0.90, water emersion lens; Olympus). Some samples were fixed with paraformaldehyde and stained simultaneously with anti-vinculin (Sigma-Aldrich) and rhodamine-labeled phalloidin as described above. Recovery experiments were done by treating cells with one of these inhibitors for 1 h and washing them with fresh medium, and the process of recovery was recorded as described above.

### Online Supplemental Material

Video 1 (supplement for Fig. 5 b) shows $Ca^{2+}$-independent contraction of model 2 stress fibers. These stress fibers contain endogenous RhoA and Rho-kinase and are able to contract when treated with $Ca^{2+}$-free Mg-ATP solution. In Video 2 (supplement for Fig. 5 c), model 1 stress fibers show $Ca^{2+}$-dependent contraction only, but they acquire $Ca^{2+}$-independent contractility when incubated with dominant-active Rho-kinase. Video 3 (supplement for Fig. 9, c–e) show confocal time-lapse recording of a GFP–actin-expressing fibroblast being treated with a Rho-kinase inhibitor, Y-27632. Note that stress fibers and the arched areas of the cell periphery gradually disappear. Nuclear relocation is also observed. In Video 4 (supplement for Fig. 9 f), the cell shown in the previous video recording was washed with fresh culture medium after 1 h of treatment with Y-27632. This time-lapse sequence shows the recovery process. Both stress fibers and arches of the cell periphery are reformed. All supplemental videos are available at http://www.jcb.org/cgi/content/full/153/3/569/DC1.

## Results

### Two Stress Fiber Models

Previously, we have published a method for isolating stress fibers from cultured cells (Katoh et al., 1998, 2000). This method is based on sequentially extracting cells with two types of detergents, first with a solution containing TEA, and then with one containing Triton X-100. $Ca^{2+}$ and Mg-ATP were required for contraction of these stress fibers (model 1). Subsequently, we found that stress fibers isolated by treating the TEA extracted cells with glycerol (model 2) could also contract. However, the time course of contraction was different between the two stress fiber models, suggesting a possibility that the two models were different in their polypeptide compositions. The immunoblotting and immunofluorescence microscopy data indicated that both stress fiber models contained all of the major stress fiber components including actin, myosin, α-actinin, and proteins associated with the focal adhesion (data not shown; Katoh et al., 1998). Fig. 1 illustrates gel electrophoresis (Fig. 1 a) and immunoblotting (Fig. 1 b), showing the presence in both models of actin, MLC, MLCK (mainly ∼130 kD short MLCK) (Lin et al., 1997,

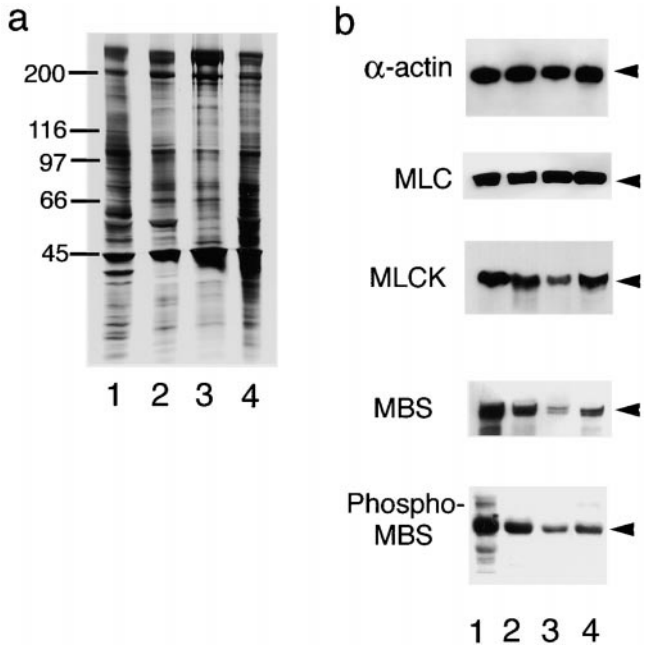


*Figure 1.* Gel electrophoresis and immunoblotting of stress fiber models with various antibodies. The whole cell extract (lane 1), Triton X-100–insoluble fraction of cells (lane 2), and model 1 (lane 3) and 2 (lane 4) stress fibers of human foreskin fibroblasts were electrophorased and silver stained (a) or immunoblotted (b) with anti–α-actin (α-actin), anti-MLC (MLC), anti-MLCK (MLCK), anti-MBS (MBS), or anti-phosphorylated MBS (phospho-MBS). Data indicate that all of these antigen polypeptides are associated with the cytoskeletal fraction and both stress fiber models. The amount of protein loaded to each lane was 2 μg for electrophoresis and 10 μg for immunoblotting.

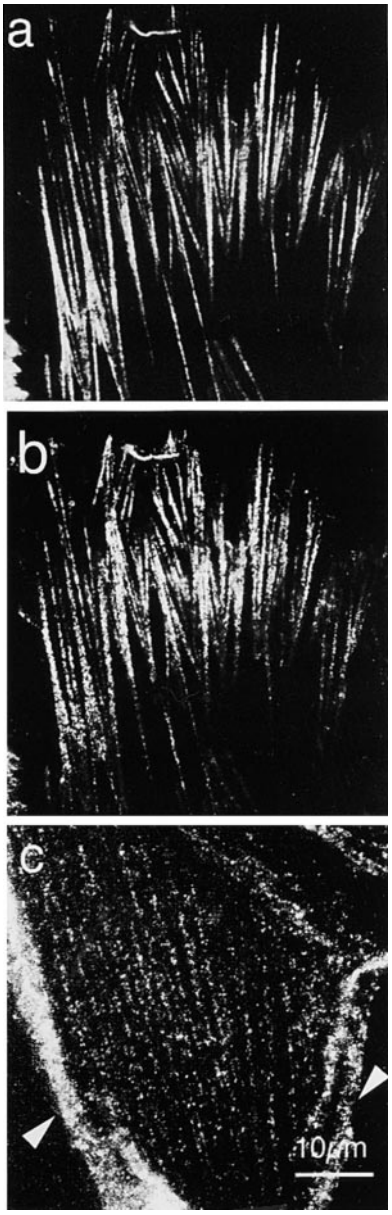


*Figure 2.* Immunofluorescence localization of myosin, MBS, and phosphorylated MBS in model 1 stress fibers. Stress fibers doubly stained with antimyosin (a) and anti-MBS (b) show dotty fluorescent patterns. When the two staining patterns were overlaid, many spots were superimposable. Banded anti–phosphorylated MBS staining is shown in c. Arrowheads in c indicate the peripheral stress fibers. Bar, 10 μm.

1999; Poperechnaya et al., 2000), MBS, and the phosphorylated form of MBS. It is interesting to note that both stress fiber models contained phosphorylated MBS.

MBS of myosin phosphatase mediates binding of this phosphatase to phosphorylated MLC. This binding enhances the activity of the catalytic subunit of myosin phosphatase that performs dephosphorylation of MLC (Alessi et al., 1992; Shirazi et al., 1994; Gailly et al., 1996). Phosphorylation of MBS inhibits the enzymatic activity of myosin phosphatase. Model 1 stress fibers that were treated with Triton X-100 for <3 min and stained simultaneously with antimyosin (Fig. 2 a, fluorescein) and anti-MBS (Fig. 2 b, rhodamine) exhibited banded staining patterns. The two banding patterns were often, but not always, superimposable. Although the staining intensity was considerably lower, antibodies against the phosphorylated form of MBS also labeled stress fibers in a spotted manner at the central portion (Fig. 2 c). This staining intensity difference between anti-MBS, and anti–phospho-MBS does not necessarily reflect the relative amounts of the two MBS forms because the anti-MBS appears to have a significantly higher affinity than the anti–phospho-MBS against respective antigens. Staining of anti-MBS and anti–phosphorylated MBS was more clearly detected at the cell periphery than the central portion. Since the peripheral stress fibers are thicker than the central ones (Katoh et al., 2001), more of these antigens are associated with the peripheral stress fibers than with the central stress fibers, and this difference may give stronger staining at the periphery.

### *Association of Rho and Rho-Kinase with Isolated Stress Fibers*

The myosin binding subunit of myosin phosphatase is a major substrate of Rho-kinase (Kimura et al., 1996). Since MBS was associated with stress fibers, we thought that Rho and Rho-kinase might also be associated with stress fibers. Cells and stress fiber models were stained with antibodies against RhoA and Rho-kinase. To ascertain that

Rho-kinase localization is not epitope-dependent, we used two different antibodies against Rho-kinase: one against the CC domain (anti-CC) and the other against the RB domain (anti-RB). When paraformaldehyde-fixed and Triton X-100–permeabilized fibroblasts were immunostained with anti-RhoA or anti–Rho-kinase, stress fiber staining was not easily detected. However, using a confocal laser scanning microscope, we observed stress fiber staining with anti–Rho-kinase (Fig. 3 a). In no case did we observe negatively stained (i.e. exclusion of immunostaining) stress fibers, indicating that Rho-kinase is not excluded from stress fibers. The difficulty of detecting stress fiber staining by these antibodies is largely due to equally strong staining of the general cytoplasm. When cells were mildly extracted, stress fiber staining with anti–Rho-kinase was easily observed by using a conventional fluorescence microscope, although there was still a considerable level of general cytoplasmic staining (Fig. 3 b).

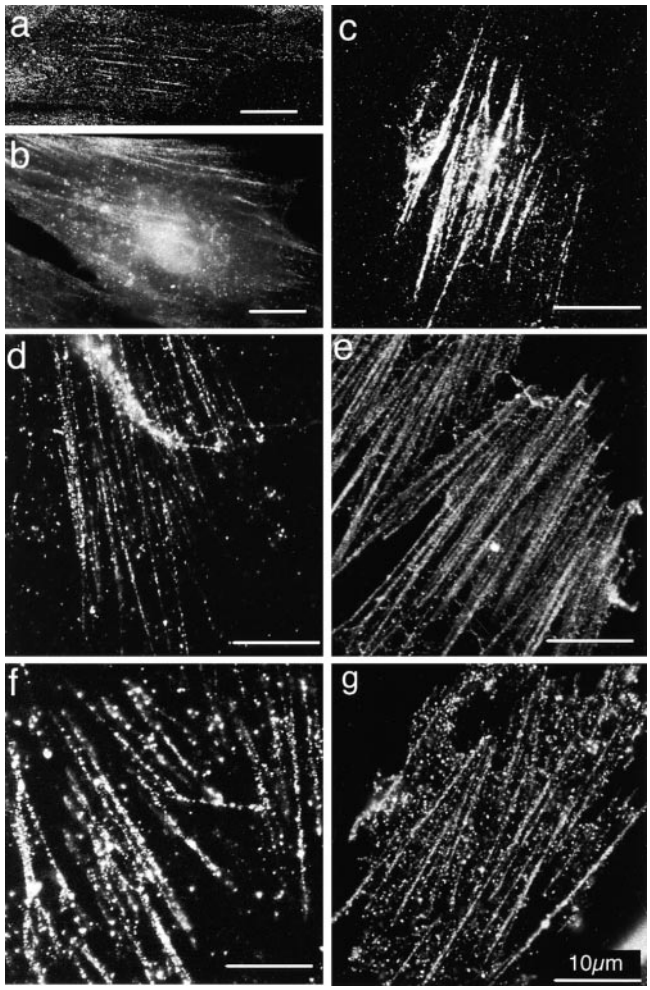


*Figure 3.* RhoA and Rho-kinase association with stress fibers. (a) A confocal image of stress fibers stained with anti–Rho-kinase (CC). The specimen was stained after the standard immunofluorescence procedure. (b) Cells were briefly extracted with Triton X-100 and stained with anti–Rho-kinase (CC). Using an epifluorescence microscope, stress fiber staining was detected against cytoplasmic staining. (c–e) Model 1 stress fibers treated with Triton X-100 for <3 min were stained with anti-RhoA (c) and anti–Rho-kinases, CC (d) and RB (e). Dotty staining along stress fibers was noted. (f and g) Model 2 stress fibers showed the similar dotted staining pattern with anti-RhoA (f) and anti–Rho-kinase (RB) (g). Bars, 10 μm.

Model 1 stress fibers treated with Triton X-100 for <3 min were stained with anti-RhoA (Fig. 3 c) or one of the two anti–Rho-kinases, anti-CC (Fig. 3 d) or anti-RB (Fig. 3 e). All of these antibodies stained the stress fiber model in a banded manner. The intensity of staining tended to taper off toward the ends of each stress fiber, and these proteins were not associated with focal adhesions. The same localization pattern was observed in model 2 stress fibers (Fig. 3, f and g). Anti-RhoA antibodies absorbed with RhoA peptide failed to stain the stress fiber models. None of the secondary antibodies used stained stress fiber models. These controls indicate that our immunostaining results are not artifacts.

For model 2 stress fibers, the pattern and intensity of anti-RhoA and anti–Rho-kinase staining did not change even with prolonged extraction by glycerol. However, for model 1 stress fibers, the immunostaining intensity by these antibodies decreased rapidly as the extraction time by Triton X-100 was increased. Extraction of RhoA and Rho-kinase by Triton X-100 is shown by immunoblotting experiments using model 1 stress fibers treated with Triton

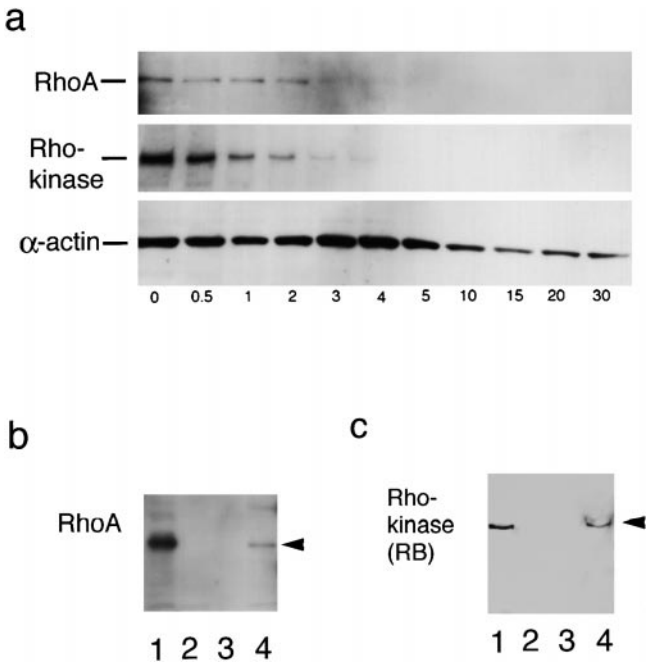


*Figure 4.* Extraction of RhoA and Rho-kinase from cells and stress fibers by Triton X-100. (a) Model 1 stress fibers were exposed to Triton X-100 for varying lengths of time (indicated in min) and analyzed for the content of RhoA and Rho-kinase by immunoblotting. RhoA and Rho-kinase were no longer detectable after 5 min of extraction. (b) RhoA, detectable in the whole cell extract (lane 1), could not be detected in the cell extracted by Triton X-100 for 10 min (lane 2). Although RhoA was not detected in model l stress fibers that were treated with Triton X-100 for 10 min (lane 3), it was associated with model 2 stress fibers (Lane 4). (c) Under these same experimental conditions, Rho-kinase was similarly extracted by Triton X-100. (a) Same amounts of TEA-treated samples were exposed to Triton X-100 for varying lengths of time. (b and c) 10 μg of proteins were loaded in each lane.

X-100 for varying length of time (Fig. 4 a). Both RhoA and Rho-kinase were present in the sample collected after TEA extraction, but they were rapidly extracted during incubation with Triton X-100 solution. After 5 min, these proteins were no longer detectable in the stress fiber fraction. Fig. 4 b shows the presence of RhoA in whole cell extracts (lane 1) and model 2 stress fibers (lane 4), but not in model 1 stress fibers extracted with the Triton X-100 buffer for 10 min (lane 3). When cells were treated with a solution containing Triton X-100 for 10 min, RhoA was not detected in the remaining cytoskeletal fraction (lane 2). The similar results were obtained when we analyzed the same samples for Rho-kinase (Fig. 4 c). Our results clearly show that both RhoA and Rho-kinase are extracted from stress fibers by Triton X-100 within 5 min. Thus, we used such stress fibers to determine the role of Rho-kinase in stress fiber contraction.

### *Stress Fiber Contraction*

Model 1 stress fibers are essentially the same as those we have made in our previous study (Katoh et al., 1998). They contracted when Mg-ATP was added in the presence of $Ca^{2+}$ and failed to do so when $Ca^{2+}$ was removed (i.e., 2 mM EGTA added). Although model 1 stress fiber contraction depended on $Ca^{2+}$, model 2 stress fibers were able to contract independent of $Ca^{2+}$ (Fig. 5 b). Since the most obvious difference between the two stress fiber models was the presence (model 2) or absence (model 1) of RhoA and Rho-kinase (Fig. 4), we exogenously added dominant-active Rho-kinase, which is composed of only the catalytic domain without the RhoA binding domain of the molecule, to model 1 to see if the stress fibers could gain contractility without $Ca^{2+}$. Indeed, as shown in Fig. 5 c, these stress fibers contracted when Mg-ATP was added in the absence of $Ca^{2+}$. Consistent with this experimental result is that model 1 stress fibers extracted with Triton X-100 only for <3 min were able to contract in the absence of $Ca^{2+}$, whereas the same model extracted for 10 min could not contract in the $Ca^{2+}$-free condition. As shown in Fig. 4 a, stress fibers extracted for <3 min, but not those extracted for >5 min, contain endogenous RhoA and Rho-kinase, and we suggest that this is the reason for the observed $Ca^{2+}$-independent contraction of the model 1 stress fibers. These results suggest that Rho-kinase plays an important role in the $Ca^{2+}$-independent stress fiber contraction (supplemental videos are available at http://www.jcb.org/cgi/content/full/153/3/569/DC1).

### *MLC Phosphorylation*

The level of MLC phosphorylation is regulated in part by myosin phosphatase, which is controlled by Rho-kinase. By phosphorylating MBS of myosin phosphatase, Rho-kinase inhibits the phosphatase activity of this enzyme. Using anti-MBS and anti–phospho-MBS in immunoblotting assays, we investigated the phosphorylation state of MBS under various conditions. For each gel, the same amount of total protein (10 μg/lane) was applied. Immunoblots with anti-MBS indicated that the amount of MBS in each sample was practically identical (Fig. 6 a). The levels of phosphorylated MBS were quantified by densitometry (Fig. 6 b). Model 1 stress fibers contained only a low level of phospho-MBS (Fig. 6, model 1, lane 1), suggesting that myosin phosphatase is active. When active Rho-kinase was added to model 1 stress fibers with Mg-ATP, MBS phosphorylation occurred (Fig. 6, model 1, lane 2), and the stress fibers contracted. This phosphorylation was significantly inhibited by Y-27632, a Rho-kinase inhibitor (Fig. 6, model 1, lane 3). MBS phosphorylation did not increase during stress fiber contraction induced by $Ca^{2+}$ and Mg-ATP (Fig. 6, model 1, lane 4).

Model 2 stress fibers contained a higher level of phospho-MBS than did model 1 (Fig. 6, model 2, lane 1). It is likely that endogenous RhoA and Rho-kinase in model 2 stress fibers are responsible for this increased level of phospho-MBS. Addition of Mg-ATP without $Ca^{2+}$ to these stress fibers increased MBS phosphorylation (Fig. 6, model 2, lane 2) and induced their contraction. The observed phosphorylation and contraction were inhibited by the Rho-kinase inhibitor (Fig. 6, model 2, lane 3). When stress fiber contraction was observed, increased MBS phosphorylation was detected in two out of three cases. Thus, inhibition of myosin phosphatase alone cannot induce reactivation of isolated stress fibers, although it is reasonable to assume that this inhibition will work in favor of contraction. Association of MBS with the stress fiber models was independent of its phosphorylation state.

As described above, model 1 stress fiber contracted in the absence of $Ca^{2+}$ if both Rho-kinase and Mg-ATP were added. Using this system, we investigated if stress fiber contraction was due to Rho-kinase's inhibitory effect on myosin phosphatase. If this were the case, other phosphatase inhibitors should also induce model 1 stress fiber contraction. Microcystin LR is a phosphatase inhibitor often used to inhibit myosin phosphatase. Model 1 stress fibers were treated with 10 μM microcystin LR, and Mg-ATP was added in the absence of $Ca^{2+}$. The stress fiber did not contract, indicating that inhibition of myosin phosphatase by Rho-kinase was not the mechanism for the reactivation of model 1 stress fibers by Rho-kinase.

Using a urea gel system, we investigated the phosphorylation state of MLC in isolated stress fibers. Fig. 7 a shows that isolated model 1 stress fibers (Triton X-100 extraction time: 20 min) contain an undetectable level of phosphorylated MLC (lane 2). When they were treated with Mg-ATP in the presence of $Ca^{2+}$, they contracted and, at the same time, phospho-MLC became detectable (lane 3). Fig. 7 b shows that isolated model 2 stress fibers also do not contain detectable level of phosphorylated MLC (lane 1). When they were treated with Mg-ATP in the presence (lane 2) or the absence (lane 3) of $Ca^{2+}$, contraction was observed and phospho-MLC was detected in both cases. By the gel shift detection, we did not detect the diphosphorylated form of MLC in stress fibers under any reactivation conditions. It appears, therefore, that stress fiber contraction is caused by phosphorylation of Ser19 in MLC. The amount of proteins loaded onto each lane was controlled to 10 μg/lane. These experiments indicate that MLC is essentially unphosphorylated in isolated stress fibers in both models and that contraction is induced by MLC phosphorylation.

Also, we investigated the phosphorylation state of MLC under various conditions using autoradiography with [$\gamma$-$^{32}$P]ATP and correlated the results with stress fiber con-

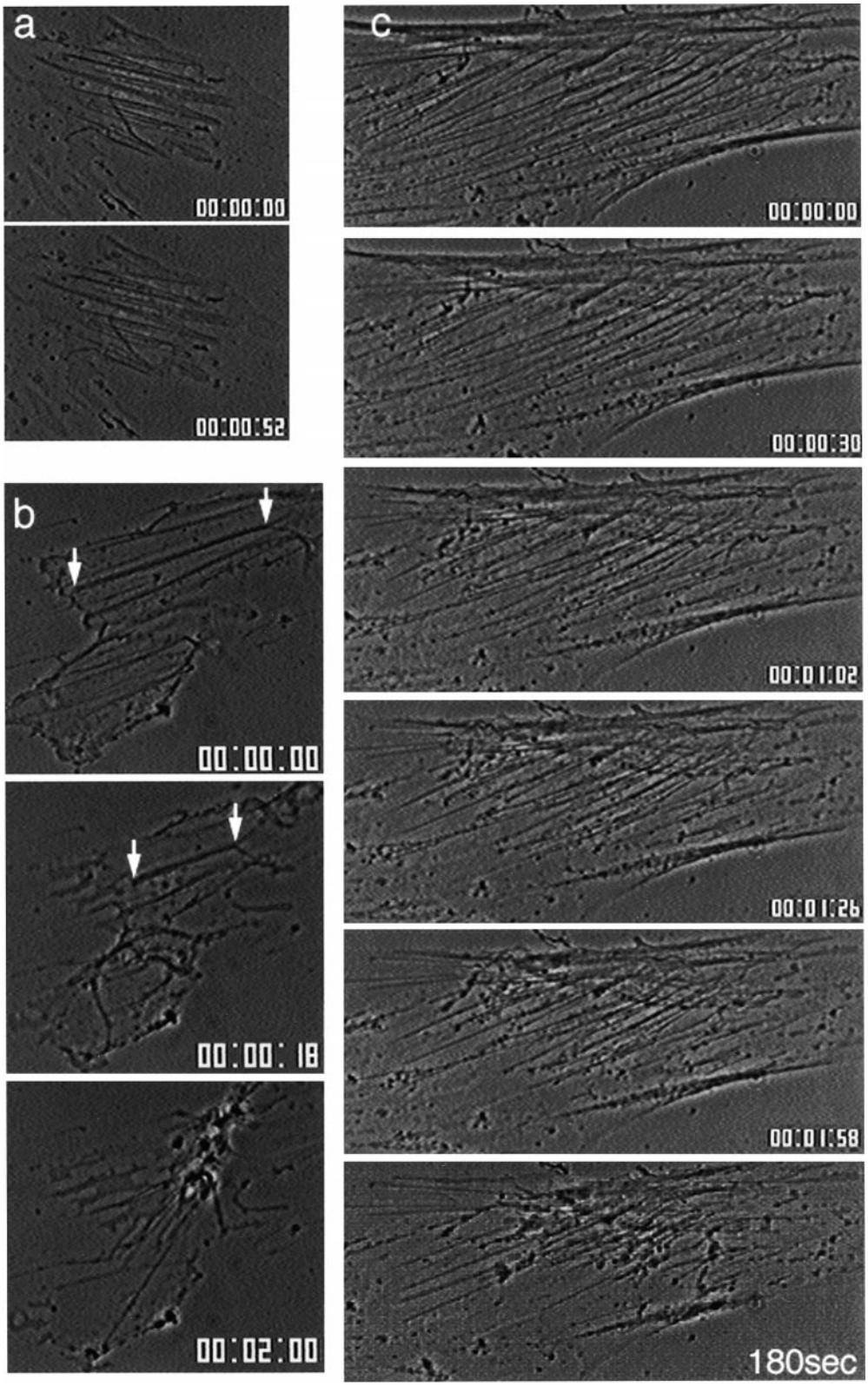


*Figure 5*. $Ca^{2+}$-independent contraction of isolated stress fibers. (a) Model 1 stress fibers were unable to contract when perfused with Mg-ATP without $Ca^{2+}$. (b) Under the same condition, model 2 stress fibers contracted (arrows). (c) Model 1, incubated with 5.1 μg/ml of dominant-active Rho-kinase, was exposed to Mg-ATP without $Ca^{2+}$. Active contraction was observed. Time (h:min:s) is shown at the bottom right side in each micrograph.

traction. The position of the MLC band on an SDS gel was determined by immunoblotting using anti-MLC and also from the band position of purified smooth muscle MLC (data not shown). The amount of protein applied to each lane was identical (Fig. 7, c–f; 20 μg/lane). MLC in model 1 stress fibers was phosphorylated when $Ca^{2+}$ was added (Fig. 7 c, lane 1), but in its absence, the phosphorylation level was greatly reduced and no stress fiber contraction was detected (Fig. 7 c, lane 2). Since $Ca^{2+}$ requirement is a characteristic feature of MLCK, the Triton X-100 extracted stress fibers were incubated first with 10 μM wortmannin, an inhibitor of MLCK, for 30 min and then with Mg-ATP.

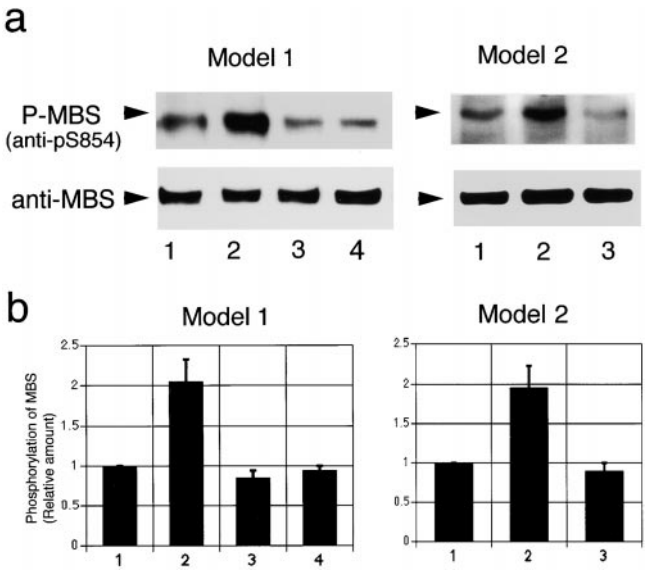


*Figure 6.* MBS phosphorylation in isolated stress fibers. (a) The phosphorylation levels of MBS in models 1 and 2 (top) are shown. The level of MBS phosphorylation in freshly isolated stress fibers was low in general in model 1 (model 1, lane 1), but it was clearly detectable in model 2 (model 2, lane 1). When model 1 stress fibers were incubated with $Ca^{2+}$-free Mg-ATP and 5.1 μM constitutively active Rho-kinase, MBS was phosphorylated (model 1, lane 2). This phosphorylation was inhibited by Y-27632 (10 μM) (model 1, lane 3). No increase in MBS phosphorylation occurred during model 1 stress fiber contraction induced by Mg-ATP with $Ca^{2+}$ (model 1, lane 4). In model 2, the phosphorylation level of MBS increased when stress fibers were incubated with $Ca^{2+}$-free Mg-ATP (model 2, lane 2). This MBS phosphorylation was also inhibited by Y-27632 (model 2, lane 3). Phosphorylated MBS was detected by using anti-pS854. The total amount of MBS in each lane was detected by anti-MBS and was essentially identical. 10 μg of proteins were loaded in each lane. (b) Quantitative analyses MBS of phosphorylation are shown. The immunoblotted bands were quantified by densitometry. The level of MBS phosphorylation in freshly isolated samples was recorded as 1, and all the data are expressed relative to this value. Each bar represents mean ± SE of four (model 1) or five (model 2) independent experiments.

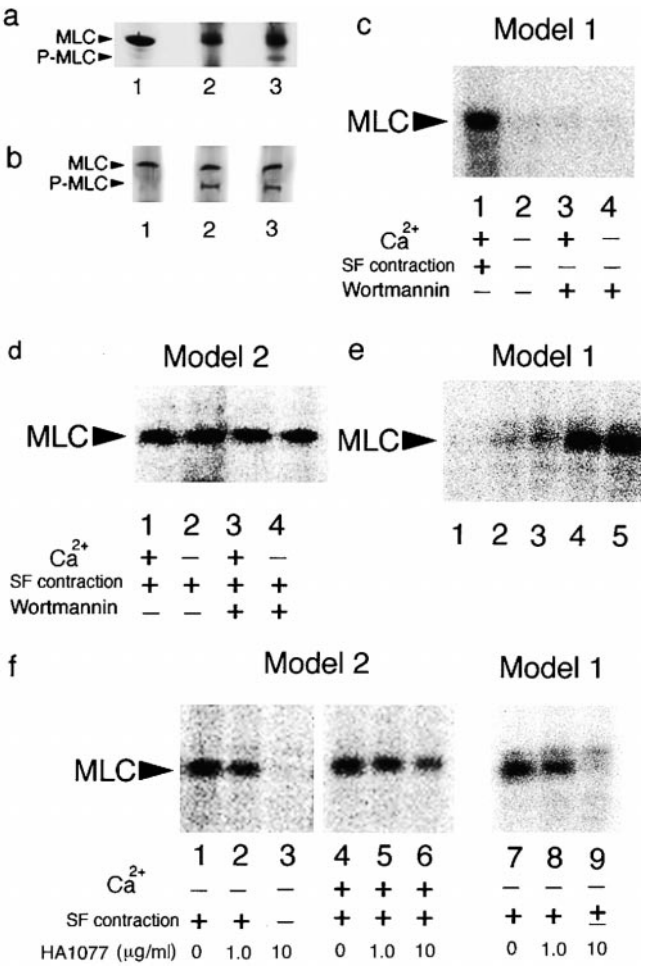


*Figure 7.* MLC phosphorylation and stress fiber contraction. MLC phosphorylation was detected by a urea gel system or autoradiography of SDS gels, and stress fiber contraction was monitored for each experimental condition under a phase–contrast microscope (+, contracted; −, not contracted). (a) Little or no phosphorylated MLC was present in freshly isolated model 1 stress fibers (lane 2). When model 1 stress fibers were treated with Mg-ATP in the presence of $Ca^{2+}$, they contracted, and phosphorylated MLC could be detected (lane 3). Lane 1 is unphosphorylated chicken gizzard MLC. (b) Little or no phosphorylated MLC was present in model 2 stress fibers (lane 1). When model 2 stress fibers were treated with Mg-ATP in the presence (lane 2) or absence (lane 3) of $Ca^{2+}$, they contracted, and MLC phosphorylated in both cases. (c) MLC phosphorylation in model 1 stress fibers was $Ca^{2+}$-dependent and was inhibited by wortmannin. Model 1 stress fibers were incubated in radio-labeled ATP with (lane 1) or without (lane 2) $Ca^{2+}$. The same samples shown in lanes l and 2 were pretreated with 10 μM wortmannin before the addition of radio-labeled ATP (lanes 3 and 4, respectively). The $Ca^{2+}$-dependent MLC phosphorylation was inhibited by the MLCK inhibitor (lane 3). (d) MLC phosphorylation in model 2 stress fibers was independent of $Ca^{2+}$ (lanes 1 and 2). The gel sample for each lane was treated in the same manner as the one shown in c. Wortmannin failed to inhibit MLC phosphorylation in model 2 (lanes 3 and 4). (e) Model 1 stress fibers were first incubated with 0 (lane 1), 0.005 (lane 2), 0.05 (lane 3), 0.51 (lane 4), or 5.1 (lane 5) μg/ml dominant-active Rho-kinase and then with radio-labeled ATP in the absence of $Ca^{2+}$. Rho-kinase concentration–dependent phosphorylation was observed. (f) Model 2 stress fibers were incubated first with 0 (lanes 1 and 4), 1.0 (lanes 2 and 5), or 10 (lanes 3 and 6) μg/ml HA1077 and then with radio-

MLC phosphorylation was inhibited both in the presence and absence of $Ca^{2+}$ (Fig. 7 c, lanes 3 and 4). Under these various conditions, model 1 stress fibers contracted only when an unequivocal level of MLC phosphorylation was detected on the gel. On the other hand, when Mg-ATP was added to model 2 stress fibers, their contraction was independent of $Ca^{2+}$ and not inhibited by the MLCK inhibitor, indicating that the contraction of this model was not mediated by MLCK (Fig. 7 d). Likewise, MLC phosphorylation occurred both with (Fig. 7 d, lane 1) and without (Fig. 7 d, lane 2) $Ca^{2+}$, and wortmannin did not inhibit these phosphorylations (Fig. 7 d, lanes 3 and 4). These data indicate that MLC in model 2 stress fibers are phosphorylated by some kinase other than MLCK. Rho-kinase is a good candidate because Kureishi et al. (1997) have recently reported that the smooth muscle MLC is phosphorylated by Rho-kinase in a $Ca^{2+}$-independent manner.

To investigate if Rho-kinase is capable of phosphorylating MLC of nonmuscle myosin, we have taken advantage of the fact that model 1 stress fibers contain essentially no

Rho-kinase. These stress fibers were first incubated with or without dominant-active Rho-kinase and then with Mg-ATP in the absence of $Ca^{2+}$. Although model 1 stress fibers were unable to spontaneously phosphorylate their own MLC (Fig. 7 e, lane 1), the light chain was phosphorylated when dominant-active Rho-kinase made as a GST fusion protein was added (Fig. 7 e, lanes 2–5). The extent of MLC phosphorylation depended on the amount of added kinase, and it was saturable (Fig. 7 e, lanes 4 and 5). The maximum level of MLC phosphorylation was achieved by 0.51 μg/ml or more of active Rho-kinase. The dominant-negative form of Rho-kinase and GST alone were unable to phosphorylate MLC (data not shown). When we monitored stress fiber contraction, the samples shown in lanes 4 and 5 always showed strong contraction.

Contraction of model 2 stress fibers occurred independent of $Ca^{2+}$. Although both MLCK and Rho-kinase are capable of phosphorylating MLC in the presence of $Ca^{2+}$, only Rho-kinase should work in the absence of $Ca^{2+}$. To ascertain that the MLC phosphorylation in model 2 stress fibers and their contraction depended on Rho-kinase when there was no $Ca^{2+}$, we pretreated these stress fibers with HA1077, another Rho-kinase inhibitor, before adding Mg-ATP. MLC phosphorylation in the absence of $Ca^{2+}$ (Fig. 7 f, lane 1) was inhibited by HA1077 in a dose-dependent manner (Fig. 7 f, lanes 2 and 3), and stress fiber contraction without $Ca^{2+}$ was inhibited by 10 μg/ml (31 μM) of HA1077 and 10 μM Y-27632. However, when the same experiments were performed in the presence of $Ca^{2+}$, both MLC phosphorylation and stress fiber contraction were not inhibited (Fig. 7 f, lanes 4–6). The MLC phosphorylation levels in lanes 5 and 6 are less than those of lane 4, but these differences did not affect the rate and extent of stress fiber contraction. Model 2 stress fiber contraction in the presence of $Ca^{2+}$ was inhibited by the addition of both wortmannin (10 μM) and HA-1077 (10 μg/ml). These results clearly demonstrate that model 2 stress fibers have two regulatory systems for contraction.

Using the reconstituting system consisting of model 1 stress fibers and dominant-active Rho-kinase, we further investigated Rho-kinase's role in MLC phosphorylation. The stress fibers were incubated with dominant-active Rho-kinase and various concentrations of HA1077 and then incubated with [γ-$^{32}$P]ATP in the absence of $Ca^{2+}$ (Fig. 7 f, lanes 7–9). The results were identical to those of the experiments using model 2 stress fibers that contained endogenous Rho-kinase.

### *Stress Fiber Contraction by MLCK and Rho-Kinase*

Model 1 stress fibers have only the MLCK system for MLC phosphorylation, and their contraction can be initi-

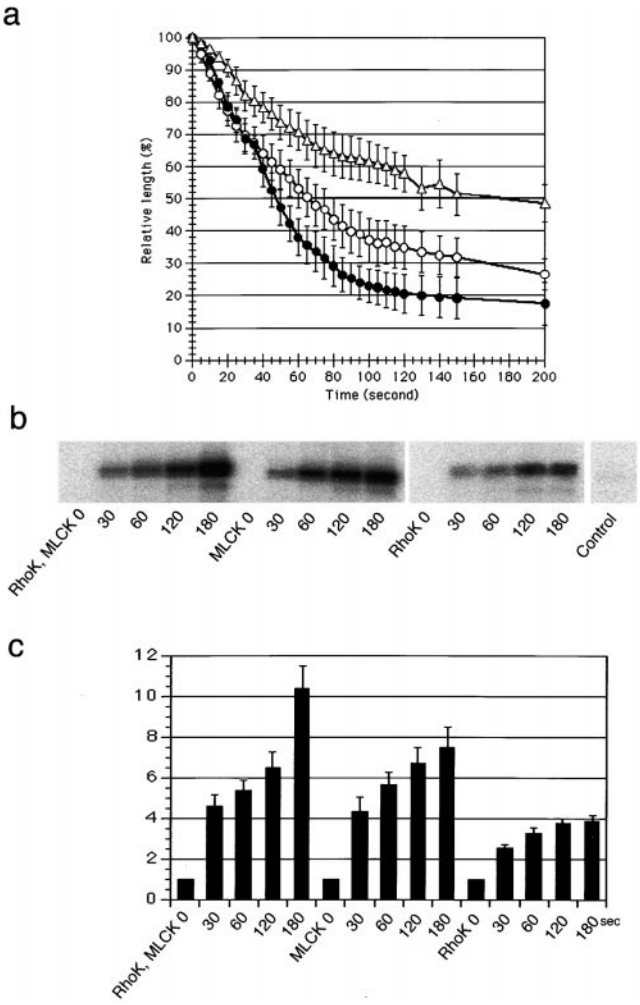


*Figure 8.* Rho-kinase and MLCK-dependent contraction of isolated stress fibers. (a) Stress fiber contraction by activating both Rho-kinase and MLCK (●), MLCK alone (○), or Rho-kinase alone (△). For details, refer to Results. The stress fiber length change expressed as a percentage of the original length was plotted against time. When both kinases were active, faster and more extensive contraction was observed. MLCK initiates contraction faster than does Rho-kinase. The values shown are means ± SE of 10 individual isolated stress fibers. (b) Time courses of the MLC phosphorylation by both Rho-kinase and MLCK, MLCK alone, and Rho-kinase alone. Phosphorylation levels were determined by autoradiography at 0, 30, 60, 120, 180 s after the addition of radiolabeled ATP. Freshly isolated stress fibers were incubated for 180 s with $Ca^{2+}$-free Mg-ATP as a control. MLC phosphorylation was comparable to the level seen at time 0 of each experiment. 20 μg of protein was loaded in each lane. (c) Quantitative presentation of MLC phosphorylation under different conditions. The autoradiography bands were quantified by densitometry. The density of the band at time 0 was recorded as 1 for each series, and all the data are expressed relative to this value. The values shown are means ± SE of four independent experiments.

labeled ATP in the absence (lanes 1–3) or presence (lanes 4–6) of $Ca^{2+}$. Without $Ca^{2+}$, Rho-kinase but not MLCK can phosphorylate MLC, and this phosphorylation was completely inhibited by 10 μg/ml HA1077 (lane 3). However, when $Ca^{2+}$ is present, both Rho-kinase and MLCK can phosphorylate MLC and the Rho-kinase inhibitor cannot inhibit MLC phosphorylation (lanes 4–6). Model 1 stress fibers were first incubated with both 5.1 μg/ml dominant-active Rho-kinase and 0 (lane 7), 1.0 (lane 8), or 10 (lane 9) μg/ml HA1077 and then with radio-labeled ATP in the absence of $Ca^{2+}$. Rho-kinase–dependent MLC phosphorylation is demonstrated. In all of these cases, stress fiber contraction was observed when MLC phosphorylation was unequivocally detected by autoradiography. (a and b) 20 μg of protein was loaded in each lane. (c–f) 10 μg of protein was loaded in each lane. (d) ±, the limited extent of contraction.

ated by adding $Ca^{2+}$ and Mg-ATP (Fig. 8 a, ○). This model could be contracted in the absence of $Ca^{2+}$ by adding dominant-active Rho-kinase and Mg-ATP. The amount of dominant-active Rho-kinase added was 5.1 μg/ml, enough to obtain the maximum phosphorylation of MLC. After the addition of ATP, stress fibers began to shorten more slowly than those contracted by activating MLCK (Fig. 8 a, △). The extent of shortening was also less than that induced by activating the MLCK system. The slower mode of contraction was observed when model 2 stress fibers were reactivated in the absence of $Ca^{2+}$ (data not shown). Model 1 stress fibers contracted more extensively in the presence of both $Ca^{2+}$ and dominant-active Rho-kinase (Fig. 8 a, ●).

To study if these different rates and extent of contraction are related to the level of MLC phosphorylation, we quantified by autoradiography the changes in MLC phosphorylation during stress fiber contraction in the three cases shown in Fig. 8 a. Both examples of the autoradiogram series (Fig. 8 b) and the densitometry data (Fig. 8 c) are shown. When both MLCK and Rho-kinase were active, the highest rate and level of MLC phosphorylation were achieved. In this case, MLCK appears to be responsible for the initial part of MCL phosphorylation, as the progression of MLC phosphorylation by both kinases was the same as that by MLCK alone. Rho-kinase's contribution becomes apparent only at the 180-s time point. These experiments demonstrate that MLCK is a much better MLC kinase than Rho-kinase, although the latter does have an MLC kinase activity.

### *Effect of Rho-Kinase Inhibitors on Living Cells*

To investigate the physiological role of Rho-kinase, we transfected GFP–actin into fibroblasts and analyzed the morphological and contractile responses of the cells to various protein kinase inhibitors. When nontransfected control fibroblasts were simultaneously stained by antivinculin (green) and rhodamine-labeled phalloidin, well-developed stress fibers and focal adhesions were present (Fig. 9 a). Y-27632 and HA1077, Rho-kinase inhibitors, significantly inhibited the expression of stress fibers and focal adhesions within 1 h (Fig. 9 b). The remaining actin bundles and adhesion points were mainly associated with the lateral cell border. Since Rho-kinase was reported to phosphorylate vimentin (Goto et al., 1998), we also checked vimentin distribution before and after Y-27632 treatment. Cells treated with Y-27632 and stained with antivimentin exhibited slightly increased vimentin filaments, but the overall distribution pattern of the intermediate filament remained unchanged before and after Y-27632 treatment (data not shown).

Fibroblasts transfected with GFP–actin developed stress fibers and exhibited the cell shape indistinguishable from nontransfected cells (Fig. 9 c). The transfected cells were treated with Y-27632 and, their behavior was monitored using a confocal time-lapse recording system for 1 h. Stress fibers gradually disappeared, and interestingly, we noted that the stress fibers that were readily dissolved were located away from the lateral cell border and that those present close to the border tended to persist longer (Fig. 9 d). We also observed that the arched region between two extended parts (Fig. 9 c, arrows and box) appeared to gradually protrude, making acute arches less acute (Fig. 9 d, arrows and box). The slow but continuous change in the shape of the arched area is illustrated in Fig. 9 e, showing gradual disappearance of the two arched regions. This local movement of the cell periphery may be explained by relaxation (i.e., loss of contractile tension) of the cytoplasm and the cortex that might be caused by inhibiting Rho-kinase. If this were the case, we might expect reappearance of the arches when the Rho-kinase inhibitor was removed. Indeed, when cells treated with Y-27632 for 1 h were washed by perfusion, some of the arches gradually deepened (arrowhead, Fig. 9 f), supporting the idea that Rho-kinase generate overall tension within the cell. Newly formed stress fibers were detected within 30 min of recovery.

As shown in Figs. 9, c and d, the overall cell shape changed little, although admittedly there were small changes associated with the cell border. However, we often observed a significant amount of nuclear dislocation in cells treated with Y-27632 (Fig. 9, c and d, dotted line). The time-lapse data indicated that the movement of the nucleus occurred in a smooth linear motion over time. Because the nuclear movement appeared to be toward the geometric center of the cell, we measured the distance between the geometric center of the nucleus and that of the cell before and l h after the Y-27632 treatment. The average distance in control cells was ~16 μm, and this distance did not change within 1 h. Interestingly, this distance decreased to ~11 μm in cells treated with the Rho-kinase inhibitor, and the change was statistically significant (Table I). This nuclear translocation towards the geometric center of the cell could also indicate general cytoplasmic relaxation (see Discussion). Other kinase inhibitors including ML-7, wortmannin, and KT5926 did not cause any of the changes described above. Fig. 9 g shows the effect of ML-7, a highly specific MLCK inhibitor (Asano, 1989). Note that stress fibers are still visible even after l h of treatment. This MLCK inhibitor tended to cause cell edges to pull in (Fig. 9 g, arrowheads), indicating that MLCK inhibition does not cause general relaxation of the cell as seen in cells treated with a Rho-kinase inhibitor. Our results appear to suggest that Rho-kinase is involved in generating tension within the cell, which is a factor for determining the overall cell shape including the off-centered position of the nucleus (supplemental videos are available at http://www.jcb.org/cgi/content/full/153/3/569/DC1).

## *Discussion*

### *Two Mechanisms for Stress Fiber Contraction*

Two stress fiber models were made. Model 1 contracted only when $Ca^{2+}$ was present, whereas model 2 contraction was $Ca^{2+}$ independent. The single most important condi-

*Figure 9.* Effects of a Rho-kinase inhibitor, Y-27632, on living fibroblasts expressing GFP–actin. Control (a) and Y-27632–treated (10 μM) (b) fibroblasts that were not transfected with GFP–actin were stained doubly with rhodamine–phalloidin (red) and antivinculin (green). Yellow indicates colocalization of these proteins. Cells treated with the inhibitor had very few, if any,

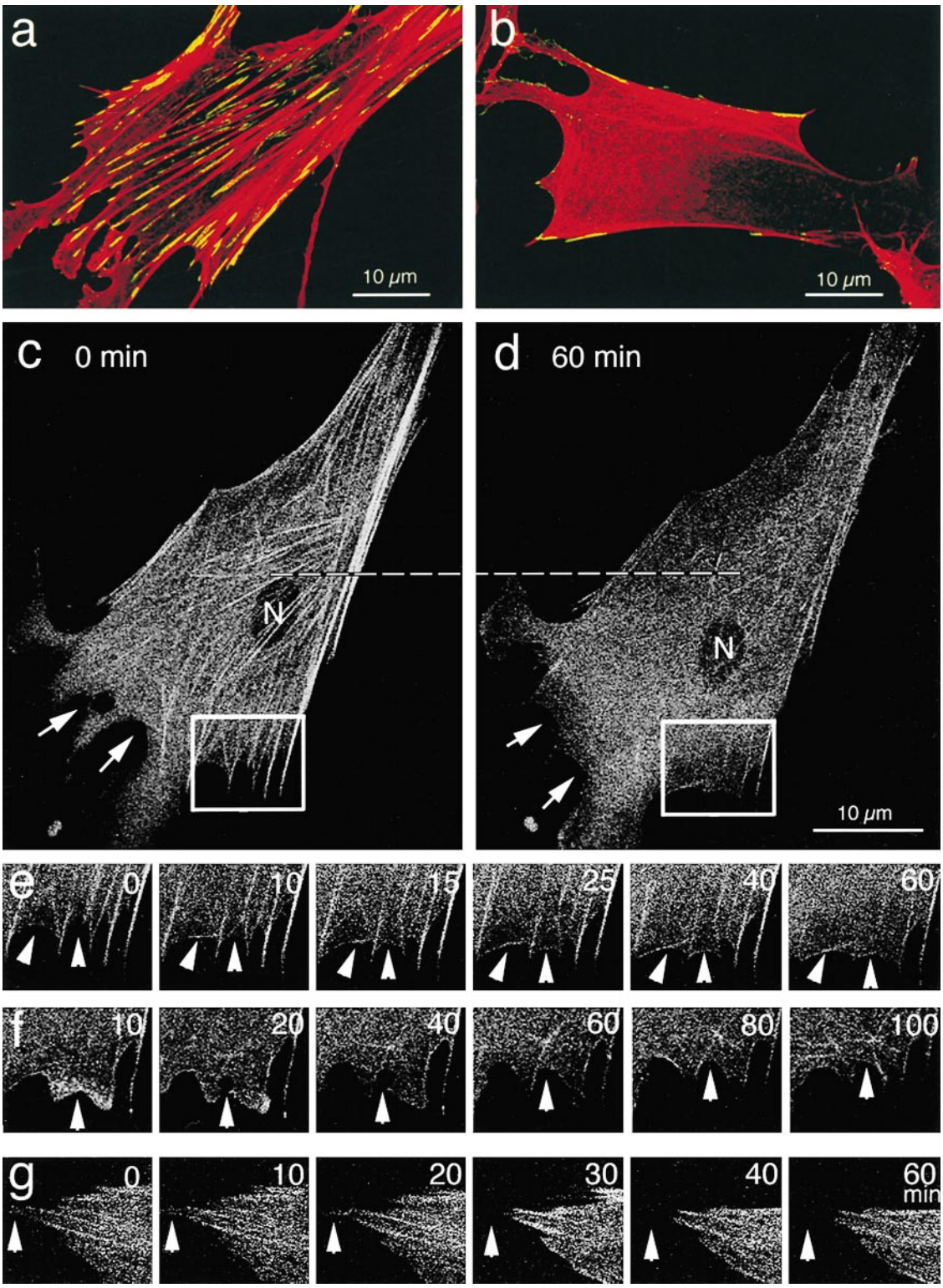


stress fibers and focal adhesions. Note the lacy appearance of the cytoplasm in the treated cells. Fibroblasts expressing GFP–actin were incubated with Y-27632, and time-lapse images were obtained by confocal laser scanning microscopy (c and d). After 1 h of incubation (d), the number and intensity of stress fibers decreased and the arches areas of the cell often disappeared (compare the boxed area in c with that of d; arrows). Nuclear relocation was also observed (the dotted line indicates the position of the nucleus before Y-27632 treatment). The boxed area in c is enlarged, and the sequence of morphological changes observed in this area is illustrated in e. Note that with time, stress fibers and arches (arrowheads) disappear. After 1 h of incubation with the Rho-kinase inhibitor, cells were washed with fresh culture medium and their recovery process was recorded (f). Both stress fibers and arches (arrowheads) reformed. These morphological changes observed in Y-27632–treated cells were not seen in cells treated with ML-7, an MLCK inhibitor (g). N, nucleus. Numbers in e–g indicate time in min.

*Table I. Distance between Geometric Centers of the Cell and the Nucleus before and after Y-27632 Treatment*

| | 0 min | 60 min |
|---|---|---|
| Control | 15.65 ± 1.75* | 15.60 ± 1.19 |
| Y-27632 | 15.92 ± 1.25 | 10.98 ± 0.94 |

The distance between the geometric center of the cell and the nucleus was determined form time-lapse recording. Measurements were made form 11 control and 19 Y-27632–treated cells that were randomly selected, and the same cells were measured at 0 and 60 min. The distance in control cells including those treated with Y-27632 for 0 min was roughly 16 μm, whereas it decreased to about 11 μm in cells treated with Y-27632 for 1 h. This decrease was statistically significant ($P < 0.05$).
*Values indicate SE.

tion for the contraction of these stress fiber models was MLC phosphorylation, and it is likely that this is true for stress fibers in the cell. Thus, the regulation of stress fiber contraction can be paraphrased as the regulation of MLC phosphorylation. MLCK is thought to be responsible for the contraction of model 1. There are several lines of evidence that support this. First and foremost, MLCK and calmodulin are localized to model 1 stress fibers (Katoh et al., 1998; this study). MLCK is activated by $Ca^{2+}$, and indeed model 1 stress fiber contraction was $Ca^{2+}$ dependent. Finally, the contraction can be inhibited by KT5926 (Katoh et al., 1998) and wortmannin (this study), which are MLCK inhibitors.

Model 2 stress fiber contraction was independent of $Ca^{2+}$ and not inhibited by the MLCK inhibitors, indicating that MLCK was not involved in this contraction. Interestingly, Rho-kinase inhibitors, such as HA-1077 and Y-27632, inhibited this contraction. These results suggest some important role played by Rho-kinase in model 2 stress fiber contraction. The Rho-kinase activity does not depend on $Ca^{2+}$, and reactivation of model 2 stress fibers was $Ca^{2+}$ independent. This study revealed that, indeed, both RhoA and Rho-kinase were present in model 2 stress fibers. Model 1 stress fibers, on the other hand, contain practically no RhoA and Rho-kinase and, therefore, do not contract in the absence of $Ca^{2+}$. However, when we added constitutively active Rho-kinase to this model, it acquired $Ca^{2+}$-independent contractility. Our data indicate that, in addition to the $Ca^{2+}$-dependent MLCK system, there is another regulatory system for stress fiber contraction involving Rho-kinase.

It is interesting to note that model 2 stress fibers contain active Rho/Rho-kinase. How this is possible is not clear, but our study highlights some intriguing facts about Rho-kinase and stress fibers. Our study showed that RhoA and Rho-kinase were associated with stress fibers, and this and other studies (Inagaki et al., 1997; Murata et al., 1997) revealed that MBS of myosin phosphatase was also associated with stress fibers. Nakai et al. (1997) have demonstrated that RhoA and Rho-kinase coimmunoprecipitated with MBS, indicating that these three proteins form a complex within a cell. Thus, it is not surprising for isolated stress fibers to contain active Rho/Rho-kinase together with MBS.

Our study showed that inactivation of Rho-kinase inside cells by specific inhibitors caused disassembly of stress fibers. Inhibitors of MLCK and other kinases, on the other hand, do not cause such disassembly. These results suggest the importance of the Rho-kinase activity for maintaining the integrity of stress fibers in the cell. However, whether or not the fraction of RhoA and Rho-kinase associated with stress fibers play major roles for maintaining the structural integrity of stress fibers is an open question. Because isolated stress fibers (model 1) can keep their integrity, albeit less stable, after both RhoA and Rho-kinase are removed, the RhoA and Rho-kinase associated with stress fibers may not be directly responsible for the maintenance of this cytoskeleton.

There are several possible schemes for the role of Rho-kinase in the reactivation of isolated stress fibers. The simplest possible mechanism is that Rho-kinase phosphorylates MLC, as Rho-kinase was shown to phosphorylate MLC in smooth muscle cells (Kureishi et al., 1997) and fibroblasts (Chihara et al., 1997; Amano et al., 1998). Thus, Rho-kinase may act as a $Ca^{2+}$-independent type of MLCK in isolated stress fibers and induce their contraction. This may indeed be the primary mechanism for the $Ca^{2+}$-free contraction of model 1 stress fibers induced by the addition of active Rho-kinase. That we detected very low levels of MLC phosphorylation in freshly isolated model 1 stress fibers is consistent with this ides. The matter, however, may not be so simple since Rho-kinase also phosphorylates MBS of myosin phosphatase and inhibits the activity of this enzyme (Kimura et al., 1996; Hartshorne et al., 1998; Iizuka et al., 1999; Kawano et al., 1999). Furthermore, the catalytic activity of Rho-kinase as an MLCK is significantly lower than that of MLCK (Amano et al., 1996a). Thus, it is possible that the Rho-kinase–induced increase of MLC phosphorylation, thus contraction, is achieved primarily by inhibiting myosin phosphatase. The less efficient phosphorylation of MLC by Rho-kinase may become sufficient when the myosin phosphatase activity is inhibited by Rho-kinase. It is interesting to note that the level of MLC phosphorylation in model 2 stress fibers did not change significantly whether or not $Ca^{2+}$ was present in the reactivation solution. It might be expected that in the presence of $Ca^{2+}$, the level of MLC phosphorylation is higher because both the MLCK and the Rho-kinase systems are active. However, our results did not indicate this to be the case. We suggest that this may be related to the fact that MLC (or myosin) is in a supramolecular assembly and not in solution. Unlike purified protein–protein interactions in solution, where every component is readily available for interaction, interaction among components in stress fibers is likely to be different. It is quite possible that a certain fraction of MLC is not readily available to enzymes. Thus, the amount of phosphorylatable MLC, not various enzymes, may be the limiting factor for the chemistry within the stress fiber. For example, in smooth muscle cells (Kureishi et al., 1997), not all MLC was phosphorylated during contraction.

A third scheme is that MLC phosphorylation is catalyzed, not by Rho-kinase, but by some unidentified $Ca^{2+}$-independent kinase(s), and such kinases could be activated by Rho-kinase or by the same condition that activates Rho-kinase. The presence of unidentified $Ca^{2+}$-independent kinases has been reported (Kureishi et al., 1997; Weber et al., 1999). SDS-PAGE of our isolated stress fiber samples shows several unidentified bands, and it is possible that one or more of these polypeptides are kinases

(Katoh et al., 1998). This last possibility needs to be investigated. Another important point to consider is that inhibition of myosin phosphatase is known to increase the $Ca^{2+}$ sensitivity of smooth muscle cells for contraction (Somlyo et al., 1999). It is less likely that this effect plays a major role in our isolated system, but when considering the situation inside cells, the increased $Ca^{2+}$ sensitivity needs to be considered.

### *Control of Nonmuscle Cell Contractility*

This study has provided direct evidence that stress fiber contraction is dually regulated. The stress fiber being regarded as a model system for the actomyosin-based contraction in nonmuscle cells, this study provides certain insights into the control for actomyosin contraction in nonmuscle cells. We suggest that the two systems are needed to obtain different modes of contraction. One type of contraction is rapid and short in duration. Such contraction may be induced by the $Ca^{2+}$/calmodulin–MLCK system and terminated by myosin phosphatase. $Ca^{2+}$ release in the cell is generally rapid and transient and is also localized. Thus, contraction triggered by $Ca^{2+}$ may be rapid, short-lived, and localized.

Another type of contraction is a sustained type. Although it would not be impossible, this type of contraction might be difficult to regulate by the $Ca^{2+}$-dependent system alone, as it will be necessary to fine tune $Ca^{2+}$ concentrations inside the cell. A sustained type of contraction may be achieved more readily by controlling the level of myosin phosphatase activity, which is done by Rho-kinase. When it is necessary to maintain certain tension in some specific areas of a cell, Rho-kinase in the region could be activated, which then phosphorylates MBS of myosin phosphatase, inhibiting the enzyme activity. In this case, it is not important how MLC has initially been phosphorylated. Once it is phosphorylated, this state can be maintained by inhibiting myosin phosphatase and contraction is also maintained in the region. It is thought that stress fibers inside cells are under isometric tension. The scheme described above is a possible mechanism for keeping the stress fiber under tension. Our data support this view as isolated stress fibers, and therefore those inside cells contain RhoA, Rho-kinase, and a detectable amount of phosphorylated MBS. During division of animal cells, the contractile ring must produce contractile force for an extended period of time. In addition to myosin (Fujiwara and Pollard, 1976), MLCK (Poperechnaya et al., 2000), and myosin phosphatase (Kawano et al., 1999), Rho-kinase has also been localized to the cleavage furrow (Takaishi et al., 1995; Kosako et al., 1999). It is possible that Rho-kinase plays a role in the prolonged generation of contractile force by this organelle.

A third type of contraction is the production of the general cytoplasmic tension. It is suggested that the balance of tension generated by the actomyosin cytoskeleton determines the three-dimensional architecture of the cell (Ingber, 1997). Cytoplasmic tension is also thought to maintain the location of various organelles and cytoplasmic compartments. By controlling the local balance between phosphorylated and unphosphorylated forms of myosin phosphatase, Rho-kinase may play an important role in generating the general cytoplasmic tension. Our immunoblot data indicate that normal fibroblasts contain both forms of this phosphatase, indicating that an appropriate balance between the active and inactive forms of myosin phosphatase is established in the cell. When cells were treated with Rho-kinase inhibitors, not only the stress fiber system disassembled, as many investigators have reported, but also dislocation of the nucleus and protrusion of arched regions of the cell periphery were observed. These effects were not caused by cell death because they were observed in living cells expressing GFP–actin and were reversible. Inhibitors for MLCK and other kinases did not induce these changes, indicating that these effects were specific for inhibiting Rho-kinase. One of the important consequences of inhibiting Rho-kinase is that there should be no further phosphorylation of MBS. In time, this would shift the active versus inactive balance of myosin phosphatase toward the active side. Without some constant signal to phosphorylate MLC, it is expected that tension generated by actomyosin contraction would become smaller. We suggest that both the nuclear relocation towards the cell center and the loss of arched areas are caused by the loss of general cytoplasmic tension in the cell. The nucleus translocation towards the cell center is only partial. This may be due to the presence of other cytoskeletal structures, especially the intermediate filaments associated with the nucleus, preventing it from moving more freely. These morphological changes are consistent, although not proofs, with the idea that Rho and Rho-kinase activity is needed to maintain the mechanical tension of the cell. Immunoblots of cell extracts with anti–phospho-MBS indicate that a certain fraction of myosin phosphatase is in an inactive form, allowing actomyosin contraction to constantly generate tension, perhaps with only a limited activity of MLCK (Fig. 10).

As described above, inhibition of Rho-kinase activity induced stress fiber disassembly and loss of cytoplasmic tension. It is not immediately clear why the loss of Rho-kinase activity induces stress fiber disassembly. Although it remains to be proven, we suggest that in order for stress fibers to maintain their structure, they must be under tension. When Rho-kinase is no longer available for providing the sustained type of contraction, stress fibers may fall apart. We have proposed that MLCK may play a minor role in providing the sustained type of contraction.

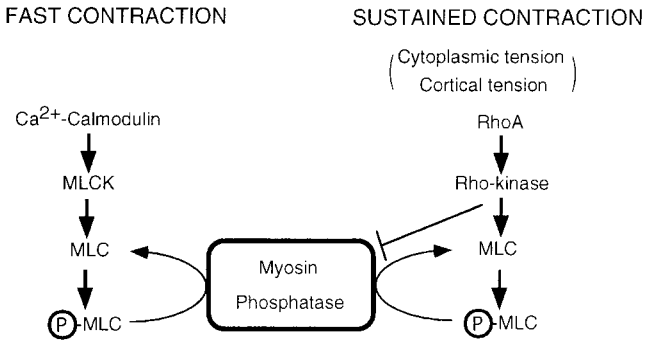


*Figure 10.* Two regulatory systems for actomyosin contraction in nonmuscle cells. P-MLC is phosphorylated MLC, which induces actomyosin-based contraction.

If this is indeed so, inhibiting MLCK may not cause stress fiber disassembly. Our experiments show that when cells were treated with MLCK inhibitors, such as ML-7, wortmannin, and KT5926, neither disassembly of stress fibers nor cell relaxation was observed. These results are in good agreement with the recent report that 3T3 cells treated with ML-9, another specific MLCK inhibitor, do not lose their stress fibers (Totsukawa et al., 2000). All these data are consistent with our hypothesis. However, Lamb et al. (1988) reported that REF-52 cells microinjected with antibodies against MLCK did lose their stress fibers without any morphological changes. It is not clear why MLCK inhibitors and anti-MLCK give different effects on the same structure, but it is possible that injected antibodies not only inhibit the MLCK activity but also affect MLCK's association with stress fibers. This latter effect may cause stress fiber disassembly.

This study has demonstrated the presence of two regulatory systems for isolated stress fiber contraction. This cytoskeletal structure being regarded as a model system for analyzing the regulatory mechanism of actomyosin-based contractility in nonmuscle cells, we suggest that these two regulatory systems are not unique to stress fibers and control other actomyosin contractile activities. Our study suggests that Rho-kinase has a critical role for the cell to generate sustained tension throughout the cytoplasm and the cortex.

We thank the two reviewers for their comments and suggestions.

This work was supported in part by grants-in-aid for Scientific Research from the Ministry of Education, Science, and Culture of Japan; grants from the Ministry of Health and Welfare of Japan; special coordination funds of the Ministry of Education, Culture, Sports, Science, and Technology of Japan; and a grant from the Organization for Pharmaceutical Safety and Research.

Submitted: 20 June 2000
Revised: 14 March 2001
Accepted: 19 March 2001

### *References*

Alessi, D., L.K. MacDougall, M.M. Sola, M. Ikebe, and P. Cohen. 1992. The control of protein phosphatase-1 by targeting subunits. The major myosin phosphatase in avian smooth muscle is a novel form of protein phosphatase-1. *Eur. J. Biochem.* 210:1023–1035.

Amano, M., M. Ito, K. Kimura, Y. Fukata, K. Chihara, T. Nakano, Y. Matsuura, and K. Kaibuchi. 1996a. Phosphorylation and activation of myosin by Rho-associated kinase (Rho-kinase). *J. Biol. Chem.* 271:20246–20249.

Amano, M., H. Mukai, Y. Ono, K. Chihara, T. Matsui, Y. Hamajima, K. Okawa, A. Iwamatsu, and K. Kaibuchi. 1996b. Identification of a putative target for Rho as the serine-threonin kinase protein kinase N. *Science*. 271: 648–650.

Amano, M., K. Chihara, K. Kimura, Y. Fukata, N. Nakamura, Y. Matsuura, and K. Kaibuchi. 1997. Formation of actin stress fibers and focal adhesions enhanced by Rho-kinase. *Science.* 275:1308–1311.

Amano, M., K. Chihara, N. Nakamura, Y. Fukata, T. Yano, M. Shibata, M. Ikebe, and K. Kaibuchi. 1998. Myosin II activation promotes neurite retraction during the action of Rho and Rho-kinase. *Genes Cells.* 3:177–188.

Amano, M., Y. Fukata, and K. Kaibuchi. 2000. Regulation and functions of Rho-associated kinase. *Exp. Cell Res.* 261:44–51.

Asano, M. 1989. Divergent pharmacological effects of three calmodulin antagonists, N-(6-aminohexyl)-5-chloro-1-naphthalenesulfonamide (W-7), chlorpromazine and calmidazolium, on isometric tension development and myosin light chain phosphorylation in intact bovine tracheal smooth muscle. *J. Pharma. Exp. Thera.* 251:764–773.

Buckley, I.K., and K.R. Porter. 1967. Cytoplasmic fibrils in living cultured cells. *Protoplasma.* 64:349–380.

Byers, H.R., G.E. White, and K. Fujiwara. 1984. Organization and function of stress fibers in cells in vitro and in situ. *Cell Muscle Motil.* 5:83–137.

Chihara, K., M. Amano, N. Nakamura, T. Yanao, M. Shibata, T. Tokui, H. Ichikawa, R. Ikebe, M. Ikebe, and K. Kaibuchi. 1997. Cytoskeletal rearrangements and transcriptional activation of *c-fos* serum response element by Rho-kinase. *J. Biol. Chem.* 272:25121–25127.

Fujiwara, K., and T.D. Pollard. 1976. Fluorescent antibody localization of myosin in the cytoplasm, cleavage furrow, and mitotic spindle of human cells. *J. Cell Biol.* 71:848–875.

Gailly, P., X. Wu, T.A.J. Haystead, A.P. Somlyo, P.T.W. Cohen, P. Cohen, and A.V. Somlyo. 1996. Regions of the 110-kDa regulatory subunit $M_{110}$ required for regulation of myosin-light-chain-phosphatase activity in smooth muscle. *Eur. J. Biochem*. 239:326–332.

Goto, H., H. Kosako, K. Tanabe, M. Yanagida, M. Sakurai, M. Amano, K. Kaibuchi, and M. Inagaki. 1998. Phosphorylation of vimentin by Rho-associated kinase at a unique amino-terminal site that is specifically phosphorylated during cytokinasis. *J. Biol. Chem.* 273:11728–11736.

Hall, A. 1998. Rho GTPases nd the actin cytoskeleton. *Science.* 279:509–514.

Hartshorne, D.J., M. Ito, and F. Erdodi. 1998. Myosin light chain phosphatase: subunit composition, interactions and regulation. *J. Muscle Res. Cell Motil.* 19:325–341.

Hoffmann-Berling, H. 1954. Adenosintriphosphat als Betriebsstoff von Zellbewegungen. *Biochim. Biophys. Acta.* 14:182–194.

Iizuka, K., A. Yoshii, K. Samizo, H. Tsukagoshi, T. Ishizuka, K. Dobashi, T. Nakazawa, and M. Mori. 1999. A major role for the Rho-associated coiled coil forming protein kinase in G-protein-mediated $Ca^{2+}$ sensitization through inhibition of myosin phosphatase in rabbit trachea. *Brit. J. Pharmacol.* 128:925–933.

Inagaki, N., M. Nishizawa, M. Ito, M. Fujioka, T. Nakano, S. Tsujino, K. Matsuzawa, K. Kimura, K. Kaibuchi, and M. Inagaki. 1997. Myosin binding subunit of smooth muscle myosin phasphatase at the cell-cell adhesion sites in MDCK cells. *Biochem. Biophys. Res. Commun*. 230:552–556.

Ingber, D.E. 1997. Tensegrity: the architectural basis of cellular mechanotransduction. *Annu. Rev. Physiol.* 59:575–599.

Isenberg, G., P.C. Rathke, N. Hülsmann, W.W. Franke, and K.E. Wohlfarth-Bottermann. 1976. Cytoplasmic actomyosin fibrils in tissue culture cells. Direct proof of contractility by visualization of ATP-induced contraction in fibrils isolated by laser microbeam dissection. *Cell Tissue Res.* 166:427–443.

Katoh, K., Y. Kano, M. Masuda, H. Onishi, and K. Fujiwara. 1998. Isolation and contraction of the stress fiber. *Mol. Biol. Cell.* 9:1919–1938.

Katoh, K., Y. Kano, and K. Fujiwara. 2000. Isolation and in vitro contraction of stress fibers. *Methods Enzymol.* 325:369–380.

Katoh, K., Y. Kano, M. Amano, K. Kaibuchi, and K. Fujiwara. 2001. Stress fiber organization regulated by MLCK and Rho-kinase in cultured human fibroblasts. *Am. J. Physiol.* 280:C1669–C1679.

Kawano, Y., Y. Fukata, N. Oshiro, M. Amano, T. Nakamura, M. Ito, F. Matsumura, M. Inagaki, and K. Kaibuchi. 1999. Phosphorylation of myosin-binding subunit (MBS) of myosin phosphatase by Rho-kinase during cell migration and cytokinasis. *J. Cell Biol.* 147:1023–1037.

Kimura, K., M. Ito, M. Amano, K. Chihara, Y. Fukata, M. Nakafuku, B. Yamamori, J. Feng, T. Nakano, K. Okawa, et al. 1996. Regulation of myosin phosphatase by Rho and Rho-associated kinase (Rho-kinase). *Science*. 273: 245–248.

Kosako, H., H. Goto, M. Yanagida, K. Matsuzawa, M. Fujita, Y. Tomono, T. Okigaki, O. Hideharu, K. Kaibuchi, and M. Inagaki. 1999. Specific accumulation of Rho-associated kinase at the cleavage furrow during cytokinases: cleavage furrow-specific phosphorylation of intermediate fileaments. *Oncogene.* 18:2783–2788.

Kreis, T.I., and W. Birchmeier. 1980. Stress fiber sarcomeres of fibroblasts are contractile. *Cell.* 22:555–561.

Kureishi, Y., S. Kobayashi, M. Amano, K. Kimura, H. Kanaide, T. Nakano, K. Kaibuchi, and M. Ito. 1997. Rho-associated kinase directly induces smooth muscle contraction through myosin light chain phosphorylation. *J. Biol. Chem*. 272:12257–12260.

Laemmli, U.K. 1970. Cleavage of structural proteins during the assembly of the head of bacteriophage T4. *Nature*. 227:680–685.

Lamb, N.J.C., A. Fernandez, M.A. Conti, R. Adelstein, D.B. Glass, W.J. Welch, and J.R. Feramisco. 1988. Regulation of actin microfilament integrity in living nonmuscle cells by the cAMP-dependent protein kinase and the myosin light chain kinase. *J. Cell Biol.* 106:1955–1971.

Leung, T., E. Manser, L. Tan, and L. Lim. 1995. A novel serine/threonine kinase binding the ras-related RhoA GTPase which translocates the kinase to peripheral membranes. *J. Biol. Chem*. 270:29051–29054.

Lin, P., K. Luby-Phelps, and J.T. Stull. 1997. Binding of myosin light chain kinase to cellular actin-myosin filaments. *J. Biol. Chem.* 272:7412–7420.

Lin, P., K. Luby-Phelps, and J.T. Stull. 1999. Properties of filament-bound myosin light chain kinase. *J. Biol. Chem*. 274:5987–5994.

Matsui, T., M. Amano, T. Yamamoto, K. Chihara, M. Nakafuku, M. Ito, T. Kanano, K. Okawa, A. Iwamatsu, and K. Kaibuchi. 1996. Rho-associated kinase, a novel serine/threonine kinase, as a putative target for small GTP binding protein Rho. *EMBO (Eur. Mol. Biol. Organ.) J.* 15:2208–2216.

Mooseker, M.S., and L.G. Tilney. 1975. Organization of an actin filament–membrane complex: filament polarity and membrane attachment in the microvilli of intestinal epithelial cells. *J. Cell Biol.* 67:725–743.

Murata, K., K. Hirano, E. Villa-Moruzzi, D.J. Hartshorne, and D.L. Brautigan. 1997. Differential localization of myosin and myosin phosphatase subunits in smooth muscle cells and migrating fibroblasts. *Mol. Biol. Cell.* 8:663–673.

Nakai, K., Y. Suzuki, H. Kihira, H. Wada, M. Fujioka, M. Ito, T. Nakano, K. Kaibuchi, H. Shiku, and M. Nishikawa. 1997. Regulation of myosin phos-

phatase through phosphorylation of the myosin-binding subunit in platelet activation. *Blood.* 90:3936–3942.

Onishi, H., M.F. Morales, K. Katoh, and K. Fujiwara. 1995. The putative actin-binding role of hydrophobic residues $Trp^{546}$ and $Phe^{547}$ in chicken gizzard heavy meromyosin. *Proc. Natl. Acad. Sci. USA.* 92:11965–11969.

Owaribe, K., and H. Masuda. 1982. Isolation and characterization of circumferential microfilament bundles from retinal pigmented epithelial cells. *J. Cell Biol.* 95:310–315.

Poperechnaya, A., O. Varlamova, P. Lin, J.T. Stull, and A.R. Bresnick. 2000. Localization and activity of myosin light chain kinase isoforms during the cell cycle. *J. Cell Biol.* 151:697–707.

Ridley, A.J., and A. Hall. 1992. The small GTP-binding protein rho regulates the assembly of focal adhesions and actin stress fibers in response to growth factors. *Cell.* 70:389–399.

Ridley, A.J., and A. Hall. 1994. Signal transduction pathways regulating Rho-mediated stress fiber formation: requirement for a tyrosine kinase. *EMBO (Eur. Mol. Biol. Organ.) J.* 13:2600–2610.

Rodewald, R., S.B. Newman, and M.J. Karnovsky. 1976. Contraction of isolated brush borders from the intestinal epithelium. *J. Cell Biol.* 70:541–554.

Shirazi, A., K. Iizuka, P. Fadden, C. Mosse, A.P. Somlyo, A.V. Somlyo, and T.A.J. Hystead. 1994. Purification and characterization of the mammalian myosin light chain phosphatase holoenzyme. *J. Biol. Chem.* 269:31598–31606.

Singer, W.D., H.A. Brown, and P.C. Sternweis. 1997. Regulation of eukaryotic phosphatidylinositol-specific phospholipase C and phospholipase D. *Annu. Rev. Biochem.* 66:475–509.

Somlyo, A.P., X. Wu, L.A. Walker, and A.V. Somlyo. 1999. Pharmacomechanical coupling: the role of calcium, G-proteins, kinases and phosphatases. *Rev. Physiol. Biochem. Pharmacol.* 134:201–234.

Sunada, H., M. Masuda, and K. Fujiwara. 1993. Preservation of differentiated phenotypes in cultured aortic endothelial cells by malotilate and phosphoascorbic acid. *Euro. J. Cell Biol.* 60:48–56.

Takai, Y., T. Sakaki, K. Tanaka, and H. Nakanishi. 1995. Rho as a regulator of the cytoskeleton. *Trends Biochem. Sci.* 20:227–231.

Takaishi, K., T. Sasaki, T. Kameyama, S. Tsukita, S. Tsukita, and Y. Takai. 1995. Translocation of activated Rho from the cytoplasm to membrane ruffling area, cell-cell adhesion sites and cleavage furrows. *Oncogene.* 11:39–48.

Takayasu, M., Y. Suzuki, M. Shibuya, T. Asano, M. Kanamori, T. Okada, N. Kageyama, and H. Hidaka. 1986. The effects of HA compound calcium antagonists on delayed cerebral vasospasm in dogs. *J. Neurosurg.* 65:80–85.

Totsukawa, G., Y. Yamakita, S. Yamashiro, D.J. Hartshorne, Y. Sasaki, and F. Matsumura. 2000. Distinct roles of ROCK (Rho-kinase) and MLCK in spatial regulation of MLC phosphorylation for assembly of stress fibers and focal adhesions in 3T3 fibroblasts. *J. Cell Biol.* 150:797–806.

Uehata, M., T. Ishizaki, H. Satoh, T. Ono, T. Kawahara, T. Morishita, H. Tamakawa, K. Yamagami, J. Inui, M. Maekawa, and S. Narumiya. 1997. Calcium sensitization of smooth muscle mediated by a Rho-associated protein kinase in hypertension. *Nature.* 389:990–994.

Van Aelst, L., and C. D'Souza-Schorey. 1997. Rho GTPases and signaling networks. *Genes Dev.* 11:2295–2322.

Watanabe, N., P. Madaule, T. Reid, T. Ishizaki, G. Watanabe, A. Kakizuka, Y. Saito, K. Nakao, B.M. Jockusch, and S. Narumiya. 1997. p140mDia, a mammalian homolog of *Drosophila* diaphanous, is a target protein for Rho small GTPase and is a ligand for profilin. *EMBO (Eur. Mol. Biol. Organ.) J.* 16: 3044–3056.

Weber, L.P., J.E. Van Lierop, and M.P. Walsh. 1999. $Ca^{2+}$-independent phosphorylation of myosin in rat caudal artery and chicken gizzard myofilaments. *J. Physiol.* 516:805–824.